A Galloping Horse Model

Hugh M. Herr and Thomas A. McMahon

The International Journal of Robotics Research 2001 20: 26
DOI: 10.1177/02783640122067255

A Galloping Horse Model

Hugh M. Herr

MIT–Harvard Division of Health Sciences and Technology
Physical Medicine and Rehabilitation
Harvard Medical School
Artificial Intelligence Laboratory
Massachusetts Institute of Technology
200 Technology Square, NE43-006
Cambridge, Massachusetts 02139 USA

Thomas A. McMahon

Division of Engineering and Applied Science
Harvard University
Pierce Hall 322
Cambridge, Massachusetts 02138 USA

Abstract

A two-dimensional numerical model of a horse is presented that predicts the locomotory behaviors of galloping horses, including how stride frequency, stride length, and metabolic rate change from a slow canter to a fast gallop. In galloping, each limb strikes the ground sequentially, one after the other, with distinct time lags separating hind and forelimb footfalls. In the model, each stance limb is represented as an ideal linear spring, and both feed-forward and feedback control strategies determine when each limb should strike the ground. In a feed-forward strategy, the first hindlimb and the first forelimb to strike the ground are phase-locked such that the time separating their adjacent footfalls is held constant by the controller. In distinction, in a feedback strategy, the footfalls of the second hindlimb and the second forelimb begin when the first hindlimb and the first forelimb are perpendicular to the model's trunk, respectively. While any limb is in contact with the ground, the controller also employs a feedback control to move each stance foot at a constant tangential velocity relative to the model's trunk. With these control schemes, the galloping model remains balanced without sensory knowledge of its postural orientation relative to vertical. This work suggests that a robot will exhibit behavior that is mechanically similar to that of a galloping horse if it employs spring-like limbs and simple feed-forward and feedback control strategies for which postural stabilization is an emergent property of the system.

KEY WORDS—horse, galloping, control, stability, legged locomotion

The International Journal of Robotics Research
Vol. 20, No. 1, January 2001, pp. 26-37,

1. Introduction

The scientific investigation into quadrupedal galloping first began in 1899 when Eadweard Muybridge presented his stop-motion photographs of galloping cats, dogs, camels, and horses (Muybridge 1899). Although Muybridge's photographs generated a great deal of interest for locomotion studies among scientists and inventors, galloping did not receive a mathematical treatment until nearly a century after the photographs were first published.

To explain why galloping is a faster quadrupedal gait than trotting, McMahon (1985) developed a simple mathematical model in which the legs of a quadruped were represented by a single massless spring and the body as a point mass. The model predicted that galloping should be 2.8 times faster than trotting. Later studies showed that this value is in reasonable agreement with experimental data[1] (Heglund and Taylor 1988), suggesting that a resonant spring-mass model can describe some galloping behaviors.

After McMahon's (1985) work, Nanua (1992) developed a two-dimensional galloping model using four massless spring-damper limbs connected to a rectangular rigid body. Unlike the passive spring-mass model of McMahon, Nanua's quadrupedal limbs were actuated and could actively shorten and lengthen as well as retract and protract.[2] To stabilize

1. On average, the lowest galloping speed was determined to be 2.6 times faster than the lowest trotting speed for 16 species of wild and domestic quadrupeds ranging in size from 30 gram mice to 200 Kg horses (Heglund and Taylor 1988).

2. Throughout this paper, *limb retraction* is defined as a backward displacement of the foot toward the quadruped's rump, by means of rotating a limb about the hip or shoulder joint within the sagittal plane. In contrast, *limb protraction* is defined as a forward displacement of the foot toward the quadruped's head (Gray 1968).

galloping in numerical simulation, he used two feedback control strategies to adjust actuator forces. In a first strategy, the total mechanical energy of the model was computed each time the model left the ground, and each leg was either shortened or extended throughout the next ground contact period to keep the model's total energy from diverging. In a second strategy, the angular position of each model limb at first ground contact was adjusted to control forward galloping speed. Although Nanua's controller did not directly stabilize model posture throughout a galloping step, his controller did require sensory information of the model's orientation with respect to vertical. Without absolute trunk position and velocity, the model's total mechanical energy could not be computed and therefore, he reasoned, could not be controlled.

Ringrose (1997) challenged the feedback control paradigm as a means of stabilizing galloping. He argued that the postural stability of a galloping machine should be inherent to its structure, not to a feedback control strategy. To support this idea, he developed a model that galloped in numerical simulation with only a feed-forward control commanding each model actuator. The model was stable without relying on sensory information of its postural orientation relative to vertical. In fact, his model could gallop without any sensory information from its environment, but its stability was dependent on the shape of each supporting limb. Ringrose used a curved foot roughly the shape of a hemisphere. When he made the foot too flat or too small, the galloping model fell over.

The mathematical models described thus far were not formulated specifically to capture the dominant mechanical behaviors of galloping animals. The models of McMahon (1985) and Nanua (1992) did not include limbs with mass or a flexible neck and back, structural features believed to be critical for realistic galloping dynamics (Alexander 1985). The model of Ringrose (1997) included large hemispherical feet not found in animals. Many mammals run on their toes, not relying on a foot platform to maintain their balance (Biewener 1989; Roberts et al. 1997). The purpose of this work is to begin to understand what control mechanisms quadrupeds might use to maintain their speed, height, and postural orientation while galloping. Do galloping animals continually measure their postural orientation relative to vertical and use this information in feedback control strategies to remain stable, or do they employ self-stabilizing feed-forward strategies to gallop steadily without relying on sensory information from their environment? We hypothesize that a robot will exhibit mechanical behavior that is similar to that of a galloping horse without the robot's postural orientation needing to be explicitly controlled or measured, not because of foot shape but because of simple feed-forward and feedback control strategies for which postural stabilization is an emergent property. To test the hypothesis, a horse model is constructed using body segment lengths and mass distributions measured from a horse. Control strategies are then formulated using horse-limb kinematic, stiffness, and morphological data. Quantitative predictions made by the model are then compared to mechanical and energetic data from galloping horses.

2. Methods

2.1. Horse Model Structure

The first research objective was to develop a horse model that was detailed enough in structure to capture the significant mechanical characteristics of galloping. To model galloping, four legs are required to show the footfall patterns of stance. Each leg must retract and protract in the sagittal plane about a shoulder or hip joint and change length about an elbow or knee joint. Furthermore, the model's neck and back should not be rigid. In slow-motion films of galloping horses, neck and back flexion can easily be observed with the eye. It is reasonable to ask whether these flexibilities are important to the overall mechanical behavior of a galloping horse.

The horse model is described in Figure 1. In a previous investigation by Herr and McMahon (2000), a model of equivalent structure was developed to study the mechanics and energetics of quadrupedal trotting. Although the structural details of this model are equivalent to the galloping model presented here, the control strategies are nonetheless distinct. As is described in Section 2.2, the footfall patterns of galloping differ from those of trotting, requiring that the control strategies of a trotting model be distinct from those necessary for the stabilization of a galloping model.

2.2. Justification of the Control Methods

2.2.1. Footfall Patterns in Galloping

Researchers refer to galloping as an in-phase gait because the same footfall pattern is repeated throughout every ground contact period in steady-state running, as opposed to trotting, an alternate gait, in which diagonal limb pairs alternately strike the ground from one contact period to the next. In galloping, the limbs strike the ground in a sequential manner. For the transverse gallop,[3] the preferred gait of horses, the ground contact phase begins when a first hindlimb strikes the ground, and then following this foot strike, a second hindlimb makes contact before or at the same time as a diagonal forelimb. And finally, after the impact of the diagonal forelimb, the second and final forelimb makes contact.

Although this basic sequence of footfalls does not change with galloping speed, the amount of time separating the foot strikes of the second hindlimb and the first diagonal forelimb increases with increasing speed (Muybridge 1899). At the slowest galloping speed, a canter gait is used in which the

3. Some animals use a rotary gallop when the sequence of footfalls goes around in a circle. Here, the first forefoot to strike the ground is on the same side of the animal as the second hindfoot. The transverse gallop is the preferred gait of horses and is therefore the gait modeled for this investigation.

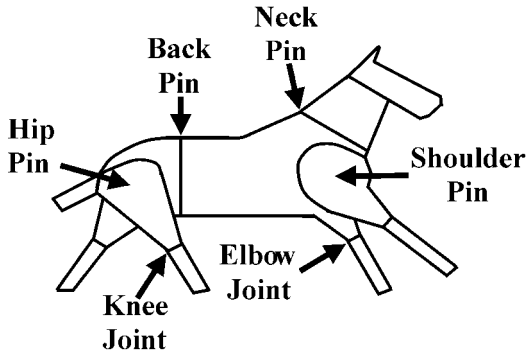

Fig. 1. The model is sketched with leg, neck, and back joints noted. There are a total of 10 degrees of freedom, 2 per leg as well as a back joint and a neck joint. All joints are rotary, except for prismatic knee and elbow joints. Three separate rigid shapes are used for the rump, body, and neck/head, and each leg is constructed with an upper rigid segment and a lower rigid segment. Mass is distributed throughout the model in a realistic manner using horse morphological data. At the distal end of each leg is a single ground contact point. The viscoelastic property of a natural running surface is modeled using springs and dampers aligned in vertical and horizontal directions. A compliant ground was required so that each model foot would not slip at first ground contact. The vertically aligned ground springs allowed each foot to penetrate the running surface, enabling the horizontal ground springs to hold the foot in place. Ground stiffness was adjusted so that the limbs only penetrated the ground by a small amount when running (∼0.3 cm). Damping was then adjusted to minimize oscillations between the ground and foot. For a detailed description of model structure, see Herr and McMahon (2000).

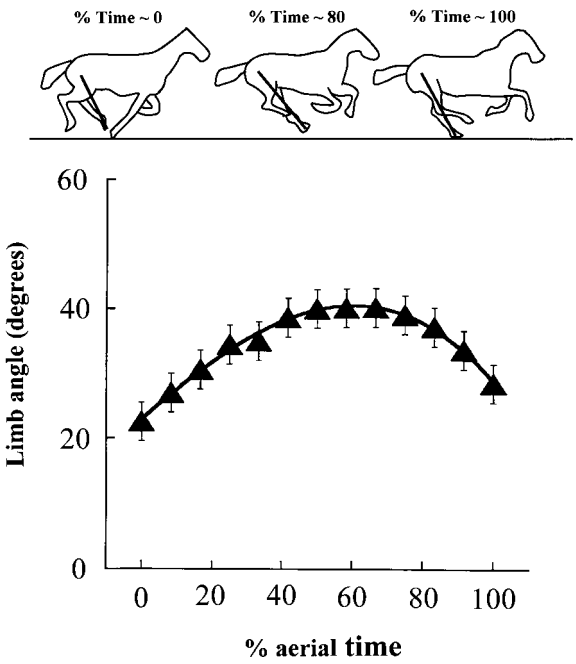

Fig. 2. The hindlimb angle of an actual galloping horse is plotted against percent aerial time. At 0% aerial time, the horse first loses contact with the ground, and at 100%, ground contact is reestablished. Video images taken at 200 frames/second were entered into the computer and then digitized for limb angle measured with respect to vertical. At approximately 80% aerial time, the first hindlimb begins to retract toward the ground. Errors are standard deviations of the mean for five consecutive gait cycles taken from one animal galloping at a steady velocity.

second hindlimb and the first diagonal forelimb contact the ground at nearly the same moment. However, at faster speeds, a time delay develops between these adjacent foot strikes. This basic trend continues until, at the maximum galloping speed, an aerial phase exists between hindlimb and forelimb ground contact phases.

2.2.2. Early Limb Retraction

In galloping, a limb can begin to retract even before striking the ground. This behavior is shown in Figure 2, in which the angle of the first hindlimb that will contact the ground is plotted against percent aerial time for a galloping horse (600 Kg). At approximately 80% aerial time, the hindlimb begins to retract toward the ground. This same behavior, retraction before striking the ground, can also be observed in the other quadrupedal limbs. Figures 3, 4, and 5 show early limb retraction in the second hindlimb, first forelimb, and second forelimb to strike the ground in a galloping sequence, respectively. Does the mechanical state of the animal trigger the retracting limb movement, or is the movement triggered by a clock or central pattern generator?

In Figure 3, the second hindlimb begins to retract approximately when the first hindlimb is vertically aligned or when the limb is approximately perpendicular with the horse's trunk. Retraction of the second forelimb, shown in Figure 5, seems to be triggered in the same manner. When the first forelimb of the horse is vertical (limb angle ∼0.0), or when the limb is approximately perpendicular with the animal's trunk, the second forelimb begins to retract toward the ground. Hence, on the basis of these data, one hypothesis of the galloping controller is that when the first contact limb of a hind- or forelimb pair is perpendicular with the trunk, retraction is triggered in the second limb.[4]

4. Alternately, a different method could be employed to trigger retraction in the second hind- or forelimb. When the first contact limb of a hind or forelimb pair first begins to lengthen from a maximally compressed state, retraction could be triggered in the second limb.

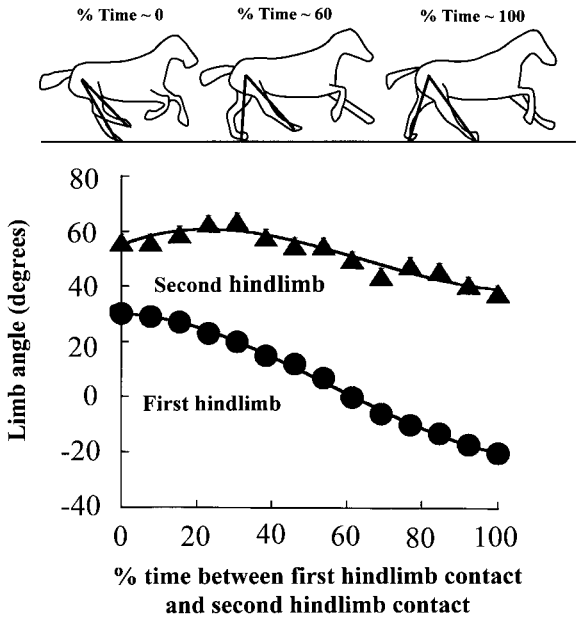

Fig. 3. Both hindlimb angles are plotted against percent time between the first and second hindlimb foot strikes. At zero percent, the first hindlimb first strikes the ground, and at 100%, the second hindlimb strikes the ground. At approximately 60%, the second hindlimb begins to retract toward the ground when the first hindlimb is approximately perpendicular with the horse's trunk (limb angle ~0.0).

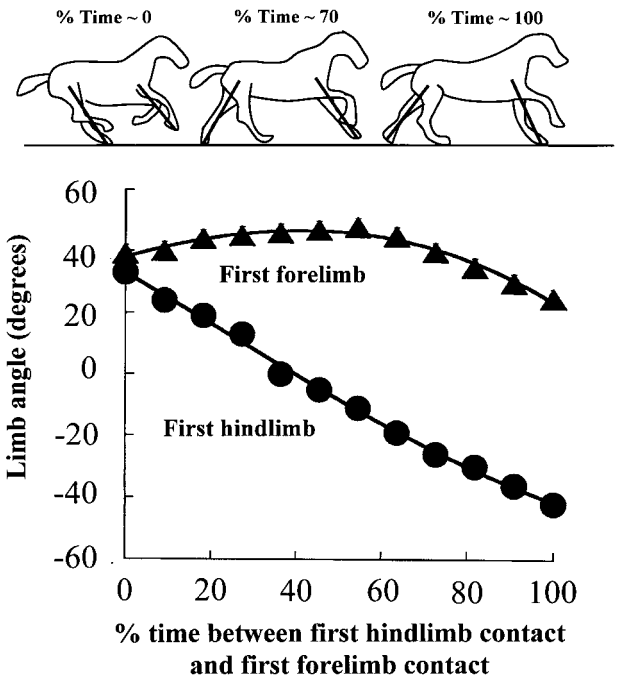

Fig. 4. The first hindlimb angle and the first forelimb angle are plotted against percent time between the first hindlimb foot strike and the first forelimb foot strike. At approximately 70%, the first forelimb begins to retract toward the ground.

Limb retraction in the first hindlimb and in the first forelimb does not seem to be triggered by the mechanical state of the animal. As mentioned previously, in the canter gait used at the slowest galloping speeds, the first diagonal forelimb strikes the ground close to the same time as the second hindlimb (Muybridge 1899). For this to occur, retraction of these limbs must nearly coincide. However, at fast galloping speeds, the first diagonal forelimb strikes the ground only after the second hindlimb has left the ground, requiring that the second hindlimb has started its retraction toward the ground long before the first diagonal forelimb even begins to retract (Muybridge 1899). Hence, the mechanical state of the hindlimbs at the point when the first diagonal forelimb begins to retract changes dramatically with galloping speed.

What could trigger the retraction of both the first hindlimb (Figure 2) and the first forelimb (Figure 4) that would work equally well at all galloping speeds? A critical hypothesis in the galloping controller is that these limbs are phase-locked. This requires that the amount of time separating the initiation of retraction in the first hindlimb and the initiation of retraction in the first forelimb is held constant by a galloping horse. In turn, the time separating the initiation of retraction in the first forelimb (during a previous ground contact phase) and the initiation of retraction in the first hindlimb is also held constant. This hypothesis requires a cycle time that changes little with speed. This is, in fact, what has been observed. In galloping animals, stride frequency typically changes by less than 10%, even though speed doubles over the galloping range (Heglund and Taylor 1988). Quadrupeds increase speed in galloping not by decreasing cycle time but by increasing the distance traveled during a cycle.

2.2.3. Elastic Structures in the Model

Throughout ground contact in galloping, each stance limb goes through a period of shortening or compression followed by a period of lengthening. Experimental evidence suggests that the vertebrate limb behaves like a spring during this period. Cavagna, Heglund, and Taylor (1977) discovered that during ground contact in running, fluctuations in forward kinetic energy of the center of mass are in phase with changes in gravitational potential energy. They hypothesized that quadrupeds most likely store elastic strain energy in tendon, ligament, and perhaps even bone to reduce fluctuations in total mechanical energy during each running step.

To represent these elastic structures in the galloping model, ideal linear springs were used to simulate limb, back, and neck behavior in stance. To model whole-limb compliance, springs were placed at knee and elbow prismatic joints (Fig. 1) so that each stance limb would go through a period of compression followed by a period of extension in a manner similar to a

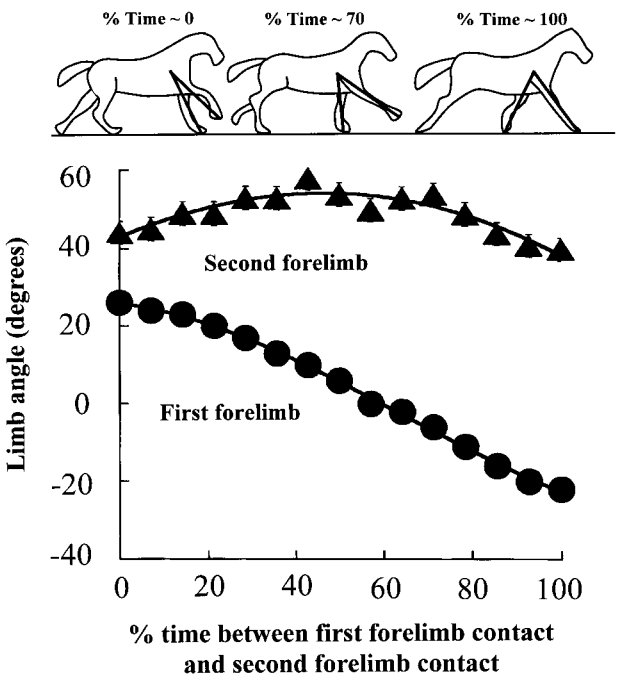

Fig. 5. Both forelimb angles are plotted against percent time between the first and second forelimb foot strikes. At approximately 70%, the second forelimb begins to retract toward the ground when the first forelimb is approximately perpendicular with the horse's trunk (limb angle ~ 0.0).

vertebrate limb. Leg springs were also used in the galloping models of McMahon (1985) and Nanua (1992) and the trotting models of McMahon and Cheng (1990) and Herr and McMahon (2000).

2.2.4. Hip Thrusting and Shoulder Braking

Of course, if all quadrupedal joints behaved as passive springs throughout stance, galloping could not be sustained, simply on the basis of energy conservation. Inspection of a horse's musculature supports the hypothesis that hip and shoulder work may be important to the maintenance of forward momentum in galloping. The preponderance of muscle mass in the hindlimb is positioned about the hip joint, acting to retract the hindlimb and to power a running step (Gray 1968). In distinction, a large fraction of forelimb muscle mass is positioned to protract the forelimb and to retard a running step. A critical hypothesis in the galloping controller advanced here is that even in constant-speed running, hip torques act as the engine of quadrupedal galloping and shoulder torques as the brake. This hypothesis is also central to the trotting horse model of Herr and McMahon (2000).

2.3. Formulation of the Control Methods

The model is two-dimensional and therefore moves only within the sagittal plane. During the aerial phase, the controller moves the hips, shoulders, back, and neck to desired angular positions relative to the model's trunk. In addition, the first hindlimb is lengthened to full leg extension for landing, and the remaining limbs are shortened for foot clearance.

Just prior to ground contact, a model limb retracts toward the ground. Depending on which limb is active, retraction begins at a particular time or at a particular limb configuration. After a fixed time interval from the initiation of retraction in the first forelimb during a previous contact period, a hip torque retracts the first hindlimb toward the ground. Retraction of the second hindlimb begins when the first hindlimb is perpendicular with the model's trunk. In addition, after a fixed time interval from the initiation of retraction in the first hindlimb, a shoulder torque retracts the first forelimb. And finally, retraction in the second forelimb begins when, once again, the first forelimb is perpendicular with the model's trunk.

All stance limbs behave as linear springs, and the tangential velocity component of each foot, measured relative to each foot's proximal hip or shoulder joint, is controlled until the limb no longer contacts the ground. While at least one hindlimb is on the ground, a linear spring acts at the model's back. Likewise, while at least one forelimb is on the ground, a linear spring acts at the neck.

During the aerial phase, conventional proportional-derivative (PD) servos are employed to position the hips, shoulders, back, and neck to desired angular positions relative to the model's trunk. PD servos are also used to lengthen the limbs for landing and to shorten the limbs for foot clearance.

To control forward running speed, torques are applied about the hip and shoulder such that the tangential velocity component of each foot, measured relative to each foot's proximal hip or shoulder joint, is sustained. Foot velocity is computed by multiplying the leg length, l, by the angular velocity of the proximal hip or shoulder joint measured relative to the trunk, $\dot{\theta}$, or

$$V_{tang} = l\dot{\theta}. \tag{1}$$

The applied torque is then proportional to the difference between a measured tangential velocity component and a target velocity, or

$$\text{Torque} = -G_v(V_{tang} - V_{target}). \tag{2}$$

The proportionality constant, G_v, is a velocity gain defining the torque response to a given velocity error. In Figure 6, the control strategies are explained in more detail using model images in a galloping sequence.

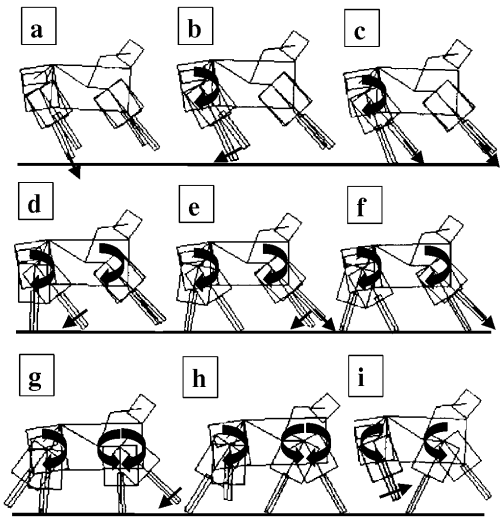

Fig. 6. The horse model is sketched in a galloping sequence. In the model images, curved arrows about the hip and shoulder joints denote directions of torque application, and straight arrows denote limb movement. During the aerial phase (a), the controller positions each limb at a protracted angle relative to the trunk. The back and neck are also positioned relative to the trunk with the back flexed in a forward position. The leg length of the first hindlimb is lengthened to full extension for landing, and the remaining limbs are shortened for foot clearance. (b) A hip torque retracts the first hindlimb foot such that its tangential velocity component, measured relative to the hip, is sustained. The limb retraction begins after a fixed time interval from the initiation of retraction in the first forelimb during the previous contact period. This velocity control continues throughout ground contact in (c) as the second hindlimb and the first forelimb lengthen for landing. When the first hindlimb is perpendicular with the model's trunk (d), the second hindlimb begins to retract and is stiffened in preparation for landing. (e) The first forelimb stiffens and begins to retract after a fixed time interval from the initiation of retraction in the first hindlimb. (f) The second forelimb continues to lengthen while the contact limbs retract against the ground. (g) The compressed first forelimb is perpendicular with the trunk, triggering retraction of the second forelimb toward the ground. At this time, the second forelimb also stiffens before striking the ground (h). When the hindlimbs or the first forelimb loses contact with the ground (i), the limbs are shortened for foot clearance and moved to protracted positions relative to the body. All the limbs behave as linear springs throughout ground contact, and the tangential velocity component of each foot, measured relative to each foot's proximal hip or shoulder joint, is controlled until the model leaves the ground. If the target hindlimb velocity (V_{target} in eq. (2)) is greater than the forward model velocity, and the target forelimb velocity is less than the forward velocity, thrusting torques are generally applied at the hips and braking torques at the shoulders, even for constant speed galloping.

2.4. Simulation Experiments

2.4.1. Numerical Methods

Physically realistic computer simulations were used to study the forces and motions of galloping. The simulations obeyed the laws of Newtonian physics as applied to trees of rigid bodies coupled together by joints. A commercially available modeling package called SD-Fast (Rosenthal and Sherman 1986) produced the simulation dynamics by generating the equations of motion and then solving them numerically using a fourth-order Runge-Kutta integration method. The equations were integrated forward at a fixed time step of 0.4 ms, while another program called Creature Library (Ringrose 1992) communicated with the controller and SD-Fast to determine the forces and torques commanded to the model's joints.

2.4.2. Velocity Range for Galloping Simulations

Analysis was not performed to determine whether galloping was the better gait, by any criterion, at a particular running speed. Rather, published observations of animal velocities were used to define the full range of galloping (Heglund and Taylor 1988). Several galloping velocities were examined, ranging from a slow canter at 5.0 meters/second to a fast gallop at 7.8 meters/second.

2.4.3. Setting Parameter Values

Knee, elbow, back, and neck stiffnesses used during stance in the trotting horse model of Herr and McMahon (2000) were also used for the galloping simulations of this paper, suggesting that joint stiffness may not change appreciably when a horse transitions from a trot to a gallop. Stable galloping[5] was found at each speed using rotary back and neck stiffnesses equal to 1.7 kN-meter/rad and 1 kN-meter/rad, respectively. Stance leg stiffnesses were selected from the range 7 kN/meter to 15 kN/meter for the knee joint and 15 kN/meter to 30 kN/meter for the elbow joint. These stiffness ranges were selected because when used in the Herr and McMahon (2000) trotting model, predictions were made of the total leg stiffness region, k_{leg} = 22 kN/meter to 40 kN/meter, where trotting horses of similar body size have been observed to operate (Farley, Glasheen, and McMahon 1993). Here, total leg stiffness, k_{leg}, defined by McMahon and Cheng (1990), is the peak vertical ground reaction force F_{max} acting at mid-stance during a trot when the leg springs are maximally compressed a distance Δl, or

$$k_{leg} = \frac{F_{\max}}{\Delta l}. \tag{3}$$

5. The model was considered to be in a stable limit cycle if galloping continued for 20 running cycles without a significant change to maximum aerial height, pitch, and forward velocity (least squares regression, $p < .05$).

Unlike joint stiffness parameters, aerial PD servo position and velocity gains were not constant across the trot-gallop transition speed. However, the aerial gains, once defined at the lowest galloping speed, were not adjusted across the entire span of galloping from 5.0 to 7.8 meters/second. The gains were defined using the same methodology employed in the trotting horse model of Herr and McMahon (2000); values were adjusted until the time required to position each joint was equal to the aerial phase time, and each limb moved to its target position with zero overshoot.

Similar to the aerial gains, the hind- and forelimb gains (G_v in eq. (2)) required to sustain the tangential velocities of hind- and forelimb stance feet and the two time durations separating limb retractions in the first hind- and forelimbs, once defined at the lowest galloping speed, were not adjusted across the entire span of galloping. The only parameters that required adjustment were the four aerial hind- and forelimb target angles and the two hind- and forelimb target velocities (V_{target} in eq. (2)). For each galloping speed and set of joint stiffnesses, genetic algorithms were employed to systematically search the parameter space within specified numerical ranges for the target limb angles and the target velocities (V_{target}). Those target angles and velocities that produced stable galloping were selected, and the resulting simulation was compared to biological data (see Section 3).

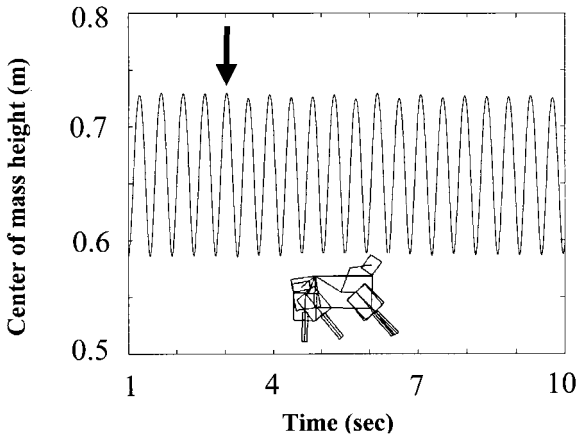

Fig. 7. The vertical height of the center of mass measured from the undeflected ground surface is plotted against time in seconds for the horse model galloping at 6.8 m/sec. At 3 seconds (denoted by arrow), when the galloping model was off the ground, the stiffness of the running surface was reduced by almost 30% from 964 kN/meter to 698 kN/meter. At 8 seconds, or 10 galloping cycles after the ground stiffness had been reduced, the model found a new stable limit cycle.

2.4.4. Disturbance Testing

Numerical experiments were conducted at each galloping speed to evaluate model stability. Such an experiment did not, in any way, serve as a proof of stability but merely suggested model robustness to a particular external disturbance. In the experiment, ground impedance was reduced but only after the model had been galloping on a stiff running surface and in a stable limit cycle. Once reduced, ground stiffness was not changed for the remaining time of simulation. With a small change to ground impedance, the model quickly recovered from the disturbance. However, when ground impedance was decreased beyond a critical level, the model could no longer remain upright on the soft surface. In each experiment, the model was considered successful in overcoming a change in ground impedance if the model found a new stable limit cycle on the softer surface. At each galloping speed, ground stiffness reductions of 20% and higher were achieved. An example of how the model responded to a ground impedance reduction of nearly 30% is shown in Figure 7. On the softer running surface, the model typically galloped with a higher stride frequency compared to the more rigid surface.

3. Results

3.1. Limb Retraction

As shown in Figures 2 through 5, each limb of a galloping horse retracts just before striking the ground. The model exhibited this same behavior in numerical simulation. The first hindlimb began to retract at a fixed time interval after retraction began in the first forelimb during a previous contact period. Similarly, retraction of the first forelimb occurred at a fixed time interval after retraction began in the first hindlimb within the same contact period. The same fixed time intervals were used for each galloping speed. The total cycle time, approximately equal to the sum of the retraction times, therefore changed little with galloping speed. The time separating retractions of the first hindlimb and the first forelimb was 37 milliseconds, and the time separating retractions of the first forelimb and the first hindlimb was 0.41 seconds.[6] These retraction times not only resulted in stable galloping but also led to good experimental predictions of total cycle time, the time between consecutive foot strikes of the same foot, and animal stride frequency, the inverse of total cycle time (see Section 3.2).

6. In this study, galloping velocity was not increased to the point where the model exhibited an aerial phase between hind and forelimb contact periods. Perhaps a future study might show that the retraction times used at slow to moderate galloping speeds fail to work at the fastest speeds, when an extended aerial phase emerges.

3.2. Overall Mechanics and Energetics of the Model

Model stride frequency was compared to experimental data taken by Heglund and Taylor (1988) on a small galloping horse (140 Kg). The results, plotted in Figure 8(a), agree with the animal data. Similar to a running horse, the model increased speed in galloping by increasing stride length, the distance traveled throughout a running cycle, not by increasing stride frequency.

Model stride length, normalized by leg length, was compared to experimental observations on horses, large cats, and dogs presented by Alexander (1977) and Cavagna et al. (1988) (Fig. 8b). The model's relative stride length increased with forward Froude number, a dimensionless velocity, in a manner similar to the galloping quadrupeds.

In addition, the model's cost of transport, the amount of metabolic energy used in moving a unit of body weight a unit distance, was compared to the cost of transport of a small running horse (140 Kg) measured in the study of Hoyt and Taylor (1981). Model predictions, shown in Figure 9, show good agreement with experimental data.

The Kram and Taylor (1990) rule was used to estimate the cost of transport using only the model's forward running speed, the average limb contact time in steady-state running, and a cost coefficient, C_o. The cost coefficient values, C_o, used to estimate the energy consumption shown in Figure 9, are listed in Table 1. Cost coefficient values were adjusted until the simulation data agreed with the experimental data. In Table 2, experimental measurements of the cost coefficient, C_o, made by Kram and Taylor (1990) are listed for three galloping speeds. The cost coefficient values in Table 1 agree well with the experimental values listed in Table 2. A complete description of how the cost of transport was computed is presented in the appendix.

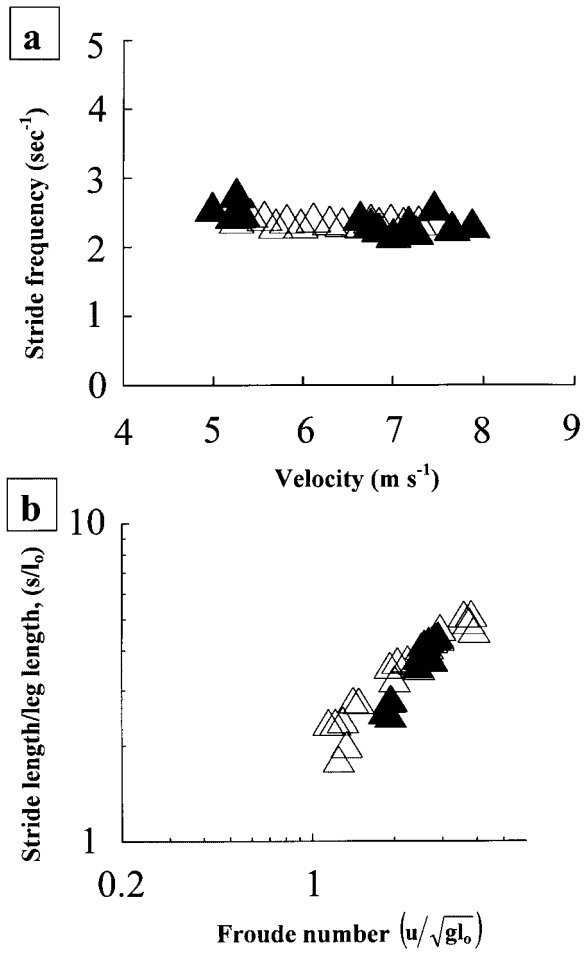

Fig. 8. (a) Stride frequency, the inverse of total cycle time, is plotted against forward speed. Open triangles are animal data from a galloping horse (140 Kg), and closed symbols are simulation results. Animal data adapted with permission from Heglund and Taylor (1988). (b) The distance the horse model moved in one complete running cycle, or the stride length, s, is normalized by the leg length, l_o, and plotted on logarithmic coordinates against the forward Froude number, $U = u/\sqrt{gl_o}$, where u is the forward velocity and g is the gravitational constant. The open symbols are animal data, and the closed symbols are simulation data. Animals represented include horses, large cats, and dogs. Animal data adapted with permission from Alexander (1977) and McMahon and Cheng (1990).

4. Discussion

4.1. Previously Developed Mathematical Models of Galloping

Two distinct control strategies have been employed to stabilize galloping models in numerical simulation. In a first strategy, the postural orientation of a quadrupedal model was

Table 1. Cost Coefficient Values Used to Estimate the Model's Cost of Transport (Fig. 9), Listed at Three Galloping Speeds (G)

Forward Speed (meters/second)	Cost Coefficient (Joules/Newton)
5.2 (G)	0.174
6.8 (G)	0.183
7.4 (G)	0.186

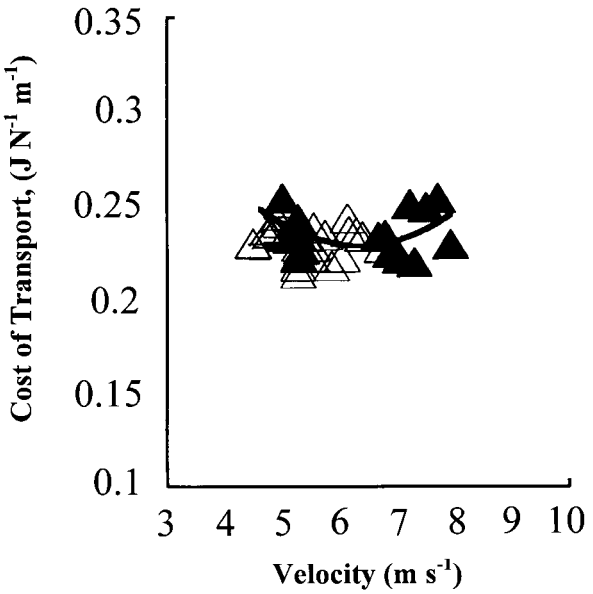

Fig. 9. The cost of transport, or the metabolic energy consumed by a running horse in moving a unit of body weight a unit distance, is plotted versus speed for the galloping horse model (135 Kg, filled symbols) and a galloping horse (140 Kg, open symbols). The experimental horse data were taken with permission from Hoyt and Taylor (1981). The Kram and Taylor (1990) rule, defined in the appendix, was used to estimate the cost of transport for the model.

Table 2. Cost Coefficient Values Listed at Three Galloping Speeds (G)

Forward Speed (meters/second)	Cost Coefficient (Joules/Newton)
5.0 (G)	0.174 ± 0.015
6.0 (G)	0.179 ± 0.007
7.0 (G)	0.184 ± 0.008

NOTE: Standard errors of the mean are included for four small horses (mean body mass = 141 Kg). Adapted from Kram and Taylor (1990); reprinted with permission.

measured relative to vertical and used to modulate actuator forces to actively stabilize galloping (Nanua 1992). In a second strategy, a quadrupedal model relied on large curved feet to ensure its balance, rather than an active control system (Ringrose 1997). In this strategy, the galloping model was stable simply because of the shape of its foot, requiring no sensory information from the environment.

Although quadrupedal models have successfully galloped in numerical simulation, their structures and movements have not specifically resembled galloping animals. The manner in which galloping animals stabilize their movement is still unknown today. In the present study, we used a numerically simulated horse model to test different control hypotheses. For acceptance of a control strategy, we required an adequate ability of the model to predict experimental observations on galloping horses not only for mechanical variables but also for the rate of energy metabolism as well.

4.2. Does the Galloping Model Have to Measure Its Postural Orientation Relative to Vertical to Remain Stable?

Our findings support the hypothesis that a horse-like robot does not require sensory knowledge of its postural orientation relative to vertical to remain balanced during steady-state galloping. The model remains stable without ever measuring or explicitly controlling absolute pitch or limb position. Stabilization does not result from an inherently stable machine structure, such as large hemispherical feet or the like. Rather, the galloping model uses both feed-forward and feedback control strategies in a distributed control scheme to stabilize pitch, speed, and height.

4.3. Why Does Controlling Relative Foot Speed Enhance Model Stability?

By sustaining the tangential velocity component of each stance foot measured relative to a proximal limb joint (see eq. (2)), the controller sustains forward speed and at the same time stabilizes body pitch. When the forelimb target velocity is smaller than the forward velocity of the galloping model and the hindlimb target velocity is greater, the shoulder generally applies a braking torque during stance and the hip a thrusting torque. This thrusting and braking behavior increases model stability by decreasing angular fluctuations in body pitch throughout stance, keeping the trunk more parallel to the ground.

In moderate to fast galloping, both hindlimbs strike the ground before the forelimbs touch down. Without a hip torque during early stance, an error in body pitch would occur by midstance, causing the shoulder to fall below the hip. This would occur for the same reason that a four-legged table would not remain upright if two of its legs were missing from one side. Without a hip torque, gravitational and inertial forces would

rotate the trunk about the hindlimbs, causing the model to nose into the ground. When a thrusting torque is applied to the hip such as in Figure 6(d), the shoulder does not fall below the hip, and the trunk remains level. The thrusting torque applies an equal and opposite torque to the trunk tending to lift the shoulder higher than the hip, countering the tendency of the model to nose into the ground.

The braking torque applied at the shoulder during late stance, as shown in Figure 6, has an opposite affect on body pitch. Braking tends to lift the hip above the shoulder, countering the gravitational and inertial forces pulling the hip downward. If both the hip and shoulder exerted thrusting torques, the hip would fall lower and lower with respect to the shoulder, destabilizing model pitch.

Braking and thrusting are also stabilizing in cantering. If a pitch error causes the hindlimb to strike the ground before the forelimb, the thrusting hip counters the gravitational and inertial forces tending to nose the model into the ground. On the contrary, if the forelimb strikes first, the braking shoulder counters the gravitational and inertial forces tending to push the hip lower than the shoulder. By adjusting the hind- and forelimb target velocities, both forward velocity and body pitch can be effectively stabilized, with the hips acting as the engine of galloping and the shoulders as the brake.

4.4. What Are the Advantages of Early Limb Retraction?

When a horse gallops at high speed, each limb begins to retract toward the ground before actually striking the ground (Figs. 2-5). The obvious advantage of early retraction is that each foot moves at zero relative velocity with respect to the ground at the moment of first ground contact. Consequently, each limb smoothly strikes the ground, thereby lowing energy losses associated with each foot collision. Another advantage of early retraction is that cycle time is controlled. When the model bounces too high in the air, the first hindlimb retracts toward the ground at a fixed time after retraction began in the first forelimb during a previous contact period. Without early retraction, the cycle time would have been increased simply because the model would have spent too much time in the air prior to striking the ground.

4.5. What Might Vestibular Sensing Be Used for in Galloping Horses?

The results of this study suggest that a horse may not have to measure body pitch using its vestibular system to remain balanced in pitch for steady-state running. If vestibular sensing is not critical to pitch stabilization in a steadily galloping horse, then what might its function be? One possibility is that the vestibular system may measure an animal's forward acceleration during a gallop, not its spatial orientation. How quickly an animal changes speed from a slow canter to a fast gallop may be an important control parameter for stabilization of velocity transients. Another possibility is that vestibular inputs are necessary for irregular terrain or for the stabilization of body roll and yaw. It is certainly the case that the vestibulo-ocular reflex is necessary to direct the eyes of an animal in any particular direction, and the vestibular apparatus, somatic righting reflexes, and the visual system itself must be employed when an animal gets up from lying on its side or rights itself in a free fall (Eyzaguirre and Fidone 1975).

4.6. How Plausible Is the Horse Model as a Biological Representation?

For acceptance of a control strategy, we required an adequate ability of the model to predict experimental observations on galloping horses of similar body size. In Figures 8 and 9, the simulation results show good agreement with experimental measurements on horses describing stride frequency, relative stride length, and the metabolic cost of transport.

Another test of model plausibility is whether the control inputs are consistent with what is known about biological sensing. The model's feedback control strategies require sensory information reporting limb ground contact, the angle and velocity of each limb with respect to the body, the length and rate of change of leg length, and back and neck joint angles. A horse could determine which of its limbs are on the ground by using either cutaneous receptors or muscle force receptors in tendons. A horse could also determine a joint's position and velocity using sensory receptors at or around the joint or in the muscle fiber that actuates the joint (Eyzaguirre and Fidone 1975).

A final plausibility test is whether model stability is sensitive to changes in ground impedance. The control scheme presented here could not be viewed as a realistic biological representation if the model were not able to overcome significant decreases in ground impedance. To test model robustness, the horizontal and vertical ground spring stiffnesses were changed in simulation experiments at three different galloping speeds (5.2 m/sec, 6.8 m/sec, and 7.4 m/sec). Without a single adjustment made to the controller, the model galloped robustly from a rigid running surface (964 kN/m) to a more compliant surface (698 kN/m) at each galloping speed (see Fig. 7).

4.7. Applications to Legged Machine Structure and Control

The information from this study may lead to an improved quadrupedal galloping machine. The most obvious advantage of the proposed method is that gyroscopic sensing may not be necessary for machine stabilization. In the proposed method, the absolute orientation of the model in space is not a required control input.

Another advantage is that a machine's legs, back, and neck would only have to behave as simple springs during stance. The horse model used back, neck, and leg spring stiffnesses that did not change appreciably with changes in forward speed. Consequently, in a galloping machine, neither force nor impedance control may be necessary at these joints.[7]

During the aerial phase, the back, neck, and legs should not behave as passive springs, simply because these joints have to be positioned in preparation for landing. But throughout stance, the joints should behave as simple springs so that the machine may rebound from the ground with each step. This joint behavior could be achieved efficiently by using a spring in series with both a low-power clutch and a small motor. During the aerial phase, the clutch would be disengaged, enabling the small motor to position the joint in preparation for landing. The clutch would then be engaged during stance to stiffen the joint with the motor exerting little to no force. With this system, most of the motor mass would be in the machine's body to actuate the shoulders and hips during stance, resulting in lightweight limbs that could easily be accelerated during locomotion.

Using the control principles outlined in this paper, it may be possible to construct a horse-like galloping robot that is dynamically stable in pitch, even without gyroscopic sensing to constantly monitor body attitude. Once constructed, such a robot would be closer in character to a simple hand-launched glider than to a helicopter in forward flight, which must be "flown" every minute to avoid a crash.

Appendix: Relevant Background Information

The Energetics of Galloping

Cross-bridge models of skeletal muscle are not used in this paper to predict directly the metabolic energy demands of quadrupedal galloping. Instead, an empirical rule is used to estimate energetic behavior using only mechanical predictions from the model. The empirical rule, presented by Kram and Taylor (1990), is based on the observation that the reciprocal of limb contact time in running increases linearly with forward speed along with metabolic rate. A useful generalization can be found by dividing the weight-specific metabolic power by the reciprocal of an animal's limb contact time to get a cost coefficient that is largely independent of animal speed and size, or

$$\frac{P_{met}}{W} = \frac{C_o}{t_c}. \qquad \text{(A1)}$$

Here, P_{met} is the metabolic power required to run, W is body weight, t_c is the average time a leg remains in contact with the ground during a running cycle, and C_o is the proportionality constant or cost coefficient. For quadrupedal mammals, the cost coefficient has an approximate value of 0.2 J N^{-1} across both speed and size.

The metabolic cost of transport, the energy to transport unit weight a unit distance, can be found from eq. (A1) by simply dividing by the animal's forward running speed u, or

$$\text{Cost of Transport} = \frac{P_{met}}{Wu} = \frac{C_o}{t_c u}. \qquad \text{(A2)}$$

In running simulations, the cost of transport is estimated by predicting how much time, on average, each limb of the galloping model remains on the ground at a particular forward speed u. Hence, for this work, the Kram and Taylor (1990) rule serves as a bridge between the mechanics and energetics of locomotion.

7. Admittedly, if ground stiffness changed dramatically and the machine could not select its own footholds, a modest level of impedance control would be required in the stance limbs, simplifying the machine greatly.

References

Alexander, R. M. 1977. Mechanics and scaling of terrestrial locomotion. In Pedley, T. J. (ed.): *Scale Effects in Animal Locomotion*. London: Academic Press, pp. 93–110.

Alexander, R. M. 1985. Elastic structures in the back and their role in galloping in some mammals. *J. Zool., Lond (A)* 207:467–482.

Biewener, A. A. 1989. Scaling body support in mammals: Limb posture and muscle mechanics. *Science* 245:45–48.

Cavagna, G. A., Franzetti, P., Heglund, N. C., and Willems, P. 1988. The determinants of the step frequency in running, trotting and hopping in man and other vertebrates. *J. Physiol.* 399:81–92.

Cavagna, G. A., Heglund, N. C., and Taylor, C. R. 1977. Mechanical work in terrestrial locomotion: Two basic mechanisms for minimizing energy expenditure. *Am. J. Physiol.* 233:R243–R261.

Eyzaguirre, C., and Fidone, S. J. 1975. *Physiology of the Nervous System.* 2d ed. Chicago: Yearbook Medical Publishers.

Farley, C. T., Glasheen, J., and McMahon, T. A. 1993. Running springs: Speed and animal size. *J. Exp. Biol.* 185:71–86.

Gray, J. 1968. *Animal Locomotion.* London: Weidenfeld & Nicolson.

Heglund, N. C., and Taylor, C. R. 1988. Speed, stride frequency and energy cost per stride: How do they change with body size and gait? *J. Exp. Biol.* 138:301–318.

Herr, H. M., and McMahon, T. A. 2000. A trotting horse model. *International J. Robotics Research* 19:566–581.

Hoyt, D. F., and Taylor, C. R. 1981. Gait and the energetics of locomotion in horses. *Nature* 292:239–240.

Kram, R., and Taylor, C. R. 1990. Energetics of running: A new perspective. *Nature* 346:265–267.

McMahon, T. A. 1985. The role of compliance in mammalian running gaits. *J. Exp. Biol.* 115:263–282.

McMahon, T. A., and Cheng, G. C. 1990. The mechanics of running: How does stiffness couple with speed? *J. Biomech.* 23:65–78.

Muybridge, E. 1899. *Animals in Motion*. London: Chapman and Hall.

Nanua, P. 1992. Dynamics of a galloping quadruped. Ph.D. diss., Ohio State University, Department of Mechanical Engineering.

Ringrose, R. 1992. The creature library: Reference guide to a C library used to create physically realistic simulations [Online]. Available: http://www.ai.mit.edu/projects/leglab/6894/handouts/cl_tutorial/cl.pdf.

Ringrose, R. 1997. Self-stabilizing running. Ph.D. diss., MIT, Department of EECS.

Roberts, T. J., Marsh, R. L., Weyand, P. G., and Taylor, C. R. 1997. Muscular force in running turkeys: The economy of minimizing work. *Science* 275:1113–1115.

Rosenthal, D. E., and Sherman, M. A. 1986. High performance multibody simulations via symbolic equation manipulation and Kane's method. *Journal of Astronautical Sciences* 34(3):223–239.